Mon. Not. R. Astron. Soc. **000**, 1–?? (2002) Printed 30 September 2015 (MN LATEX style file v2.2)

Transient C IV Broad Absorption Lines in radio detected QSOs

arXiv:1509.08471v1 [astro-ph.GA] 28 Sep 2015

M. Vivek[1⋆],R. Srianand[2] & N. Gupta[2]
[1] *Department of Physics and Astronomy, University of Utah, Salt Lake City, UT 84112, USA*
[2] *Inter University Centre for Astronomy and Astrophysics, Pune 410007, India*

Accepted . Received ; in original form

ABSTRACT

We study the transient (i.e. emerging or disappearing) C IV broad absorption line (BAL) components in 50 radio detected QSOs using multi-epoch spectra available in Sloan Digital Sky Survey DR10. We report the detection of 6 BALQSOs having at least one distinct transient C IV absorption component. Based on the structure function analysis of optical light curves, we suggest that the transient absorption is unlikely to be triggered by continuum variations. Transient absorption components usually have low C IV equivalent widths (<8 Å), high ejection velocities (> 10000 kms^{-1}) and typically occur over rest-frame timescales > 800 days. The detection rate of transient C IV absorption seen in our sample is higher than that reported in the literature. Using a control sample of QSOs, we show that this difference is most likely due to the longer monitoring time-scale of sources in our sample while the effect of small number statistics cannot be ignored. Thus, in order to establish the role played by radio jets in driving the BAL outflows, we need a larger sample of radio detected BALs monitored over more than 3 years in the QSO's rest frame. We also find that the transient phenomenon in radio detected and radio quiet BALs does not depend on any of the QSO properties i.e. the Eddington ratio, black hole mass, bolometric luminosity and optical-to-IR colours. All this suggests that transient BAL phenomenon is simply the extreme case of BAL variability.

Key words: galaxies: active; quasars: absorption lines; quasars: general

1 INTRODUCTION

Outflows in QSOs are detected as blue-shifted broad absorption line (BAL) troughs (see Weymann et al. 1991) in the optical spectrum of 20-40% of QSOs. This observed BAL incidence is interpreted as the covering factor of the BAL outflow in the orientation based models and as the duration of BAL phase in a QSO's life in the evolutionary models. Photoionization models with additional constraints on electron density allow one to determine the location of the outflow and estimate the mass outflow rate. The models suggest that the outflows carry sufficient kinetic luminosity to provide the necessary Active Galactic Nuclei (AGN) feedback often invoked in theoretical and numerical simulations to explain the observed properties of galaxies (Moe et al. 2009; Dunn et al. 2010; Bautista et al. 2010; Borguet et al. 2013). Thus, understanding the origin and physical conditions in BAL outflows is not only important for understanding physics of AGNs but also for understanding feedback associated with the galaxy evolution (Germain et al. 2009; Hopkins et al. 2009).

Radio jets and lobes are manifestations of large scale outflows of relativistic plasma from central regions of the QSOs. It is well established that by studying radio emission at different frequencies and angular scales one can statistically constrain the orientation and the age of radio sources. Therefore, radio observations of a sample of BALQSOs can in principle be used to distinguish between the evolution and orientation based models of BALs. Until recently such studies were practically impossible as the number of known radio loud BALQSOs was very small. But the situation has dramatically changed with the availability of huge spectroscopic samples of QSOs from Sloan Digital Sky Survey (SDSS). For example, by stacking radio images of BALQSOs from SDSS DR3, White et al. (2007) have shown that the BALQSOs have consistently higher radio flux densities than the non-BALQSOs. This may suggest that BALs are observed closer to the jet axis and is at odds with conventional orientation based models that require viewing angles closer to edge-on for BALQSOs. Studies involving radio spectral indices of BALQSOs have also been used to investigate the orientation

⋆ E-mail:vivekm@astro.utah.edu

of BALQSOs. These studies revealed that BALs occur both in equatorial and polar configurations i.e. there is no preferred orientation (Jiang & Wang 2003; Gregg et al. 2006; Ghosh & Punsly 2007).

Further radio observations of BALQSOs suggested that these sources are similar to compact steep spectrum sources (CSS; sizes<15 kpc) that are considered to be the young radio sources (Montenegro-Montes et al. 2009; DiPompeo et al. 2012). But it is now known that in VLBI (Very Large Baseline Interferometry) i.e. milliarcsec (mas) scale resolution imaging studies, the radio emission associated with BALQSOs is not necessarily unresolved or compact (Jiang & Wang 2003; Kunert-Bajraszewska & Marecki 2007; Liu et al. 2008; Montenegro-Montes et al. 2009; Gawronski & Kunert-Bajraszewska 2011; Bruni et al. 2012, 2013; Kunert-Bajraszewska et al. 2015). Thus, all these studies at radio wavelengths based on image stacking, spectral indices and VLBI imaging techniques suggest the presence of BAL outflows at various orientations and in various phases of the QSO evolution.

There have also been studies of variability of BALs in radio loud QSOs to understand the origin of outflows. Welling et al. (2014) investigated the C IV BAL variability using a sample of 46 radio loud QSOs and reported no correlations between BAL variability and radio properties. However, they noted that the amplitude of BAL variability is typically lower for radio loud sample compared to a radio quiet sample. Also, they found that there is a mild tendency for the lobe-dominated QSOs to show greater fractional BAL variability. These results suggest a relationship between the presence of radio jet and the BAL variability. In this context, it is interesting to ask how prevalent is the jet-cloud interaction in BALQSOs and if it also plays a major role in driving the observed absorption line variability.

The extreme cases of absorption line variability are the ones where the flow emerges afresh or shows strong dynamical evolution (i.e. variation in the absorption profile and signatures of acceleration). Probing these emerging/disappearing BAL components (denoted as "*transient BAL components*" from now on for convenience) can shed more light on to the hitherto unknown QSO outflow driving mechanisms. Vivek et al. (2012a) reported the first emerging Mg II BAL in SDSS J1333+0012 and Vivek et al. (2012b) reported the disappearance of a fine structure line BAL in SDSS J2215-0045. Filiz Ak et al. (2012) searched the SDSS-III catalog for such sources and reported 21 cases of C IV BAL trough disappearance in 19 sources. These together with previous reports on C IV BAL transients (Ma 2002; Hamann et al. 2008; Leighly et al. 2009; Krongold et al. 2010; Rodríguez Hidalgo et al. 2011) attribute them to a multiple streaming wind moving across the line of sight (Proga et al. 2012). However, most of the reported QSOs showing transient BAL absorption in the past happen to be radio quiet. This may be because past studies most often focused on radio quiet quasars for variability studies.

The objective of the present study is to understand the role played by radio jets in driving BAL outflows using a sample of radio detected BALQSOs suitable for identifying transient BAL absorption component. The sample is based on optical spectroscopic data available from the SDSS and 1.4 GHz flux densities available from the Faint Images of the Radio Sky at Twenty-cm (FIRST) survey. The FIRST radio survey provides a map of the sky at 1.4 GHz with a beam size of 5.4" and an rms sensitivity $\sim$ 0.15 mJy per beam. This manuscript is arranged as following. Section 2 describes the radio detected BALQSO sample used in this study. Section 3 describes the measurements of optical and radio properties of the sources and C IV broad absorption lines and Section 4 describes the analysis of the variability of BALs. Section 5 presents the statistical study of BALQSOs in our sample. Discussion and summary are given in Section 6. In this work, we assume a cosmology with $H_0 = 70$ km s^{-1} Mpc^{-1}, $\Omega_M = 0.3$ and $\Omega_\Lambda = 0.7$.

2 RADIO DETECTED SAMPLE OF BALQSOS

In this study, we have used spectra of BALQSOs from the SDSS Data Release-10 (DR10; Pâris et al. 2014). In addition to the previous data releases, SDSS DR10 consists of data from the recently concluded Baryon Oscillation Spectroscopic Survey (BOSS; Dawson et al. 2013). BOSS used the upgraded spectrographs with larger number of fibers per plate for obtaining the spectra. The fibers used for BOSS have better throughput and the spectra have wider wavelength coverage (i.e 3600-10,400 Å) as compared to those in SDSS I/II (i.e 3800-9200 Å).

Our initial sample consists of all the BALQSO's in the SDSS DR10 that were observed with the ancillary target bit name "VARBAL" describing photometrically-selected candidate BALQSOs. This sample of optically bright sources, with i-psf magnitude less than 19.28 mag, containing at least one moderately strong absorption in their BAL troughs, were primarily targeted to investigate BAL variability on multi-year timescales (Dawson et al. 2013). We retrieved 684 BALQSOs which have multiple epoch observations in SDSS DR10. Among these, 63 sources are radio detected as per the FIRST survey catalog with a typical detection limit of 1 mJy. From these 63, we discarded six sources[1] where the BAL presence is found to be ambiguous based on our manual check. Seven low-z QSOs[2] contain only Mg II BALs and we do not include them in the final sample. Our final sample consists of 50 FIRST radio detected BALQSO sources containing C IV BAL profiles with repeat observations in the SDSS. Table 1 lists the sources in our sample with their name, Right Ascension, Declination, emission redshift, flux density at 1.4 GHz from FIRST survey, corresponding radio luminosity, numbers of multi-epoch spectra available in SDSS, number of C IV absorption components contributing to the BAL absorption trough (see the next section for our definition of C IV components) and an 'ID' characterising variability in C IV BALs. Some useful notes are also provided in the last column of the table for individual sources.

We also obtained the continuum light curve measurements from the Catalina Real-Time Transient Survey (CRTS; Drake et al. 2009) for 48 sources in our final sample of 50 sources. CRTS operates with an unfiltered set up and the resulting magnitudes are converted to V magnitudes using the transformation equation, $V = V_{ins} + a(V)$

[1] J0040+0059, J0733+4625, J1349+3823, J1357+0055, J1509-0133, J1626+3752

[2] J0944+0625, J1149+3933, J1259+1213, J1324+0320, J1400-0129, J1523+3914, J1618+4113

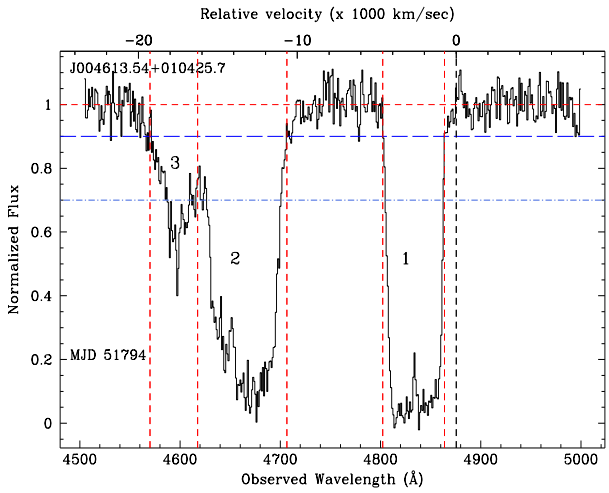

Figure 1. An example demonstrating how individual C IV components are automatically identified in our analysis. The above plot is for the source SDSS J0046+0104. Our automatic procedure first involves identifying the absorption edges where the normalized flux falls below 0.9 for 5 consecutive pixels. We further divide the identified components in to sub-components if the normalized flux rises above 0.7 continuously for 5 pixels. The velocity scale shown in the top (x-axis) is defined with respect to the C IV emission redshift, z_{em} = 2.1551. Red dashed vertical lines mark the absorption edges of the components identified.

+ b(V)*(B - V), where V_{ins} is the observed open magnitude, and a(V) and b(V) are the zero-point and the slope, respectively. The zero-point and slope are obtained from three or more comparison stars in the same field with the zero-point being of the order of 0.08 mag. The CRTS provides four such observations taken 10 min apart on a given night. Since we are mainly interested in the long-term variability, we have averaged these four points (or less if the measurement in one or more cases when the image of our object of interest is affected by some observational artifacts) to get the light curves.

3 OPTICAL CONTINUUM AND ABSORPTION LINE PROPERTIES

For all the sources in our sample, the optical properties based on absorption lines were measured from the SDSS spectra and the continuum variability properties were measured from the CRTS light curves.

We fitted all the spectra with a continuum approximated by a second order polynomial for absorption/emission free regions and Gaussians for emission lines. As we are interested mainly in studying the C IV BALs, we fitted the continuum only over a small rest wavelength range (1300 $<\lambda_{rest}(\AA) <$ 1700) relevant for the C IV and Si IV broad absorption lines. The fitting procedure involves masking the wavelength range of absorption and bad pixels, and fitting the flux in the remaining wavelength ranges with a second order polynomial and Gaussian emission lines. We used the resulting continuum to normalize the corresponding spectrum.

We then measured the C IV absorption line equivalent widths from the normalized spectra. This involves identifying the absorption edges and individual components. First, we visually inspected all the spectra to identify BALQSOs with at least one transient component. When a transient BAL component is noticed, we chose spectrum having the maximum absorption strength to identify the component structure. In the remaining cases, we have used the spectrum with the best signal to noise for this purpose. For all the spectra, wavelengths were converted to relative velocities with respect to the C IV emission redshift. Absorption edges were identified as velocities where the normalized flux falls below 0.9 continuously for 5 pixels. After this first pass, the identified components are again divided into further components if the flux rises above 0.7 continuously for 5 pixels. In this case, the mean velocity of the pixels with normalized flux values above 0.7 is taken as the absorption edge. After identifying different components and their velocity edges, we measure the equivalent widths for each components. Fig. 1 demonstrates this procedure for the source SDSS J0046+0104. The first pass identifies only two components and the second pass further divides the second component into two. Apart from the equivalent widths, we also measure the mean depth of the BAL components to characterise the strength of the absorption. Mean depth is measured by averaging the normalized flux of three pixels around the optical depth weighted velocity centroid.

We also constructed a control sample of radio quiet BALQSOs from the SDSS DR10 catalogue to quantify the role played by the radio jets in driving the transient BAL components in radio detected BALQSOs. For each of the six quasars exhibiting transient BAL components in our sample (see next Section), we obtained 10 radio quiet BALQSOs matching closely in the absolute i-band magnitude and redshift.

4 VARIABILITY OF BALS: ANALYSIS AND RESULTS [3]

We visually checked all the available spectra of individual sources for C IV absorption line variations by overplotting different epoch spectra. Optical depth variability in C IV BALs are detected in several sources in our sample without showing large variations in the velocity profile. However, in six sources, we see dramatic variations in the BAL profiles. In the latter epochs of these sources, either a new velocity component has emerged afresh or an already existing component has completely disappeared.

Fig. 2 shows the normalized spectra of these six sources showing C IV BAL transient components. Red dashed spectra correspond to later epoch measurements. Horizontal blue dashed line corresponds to the unabsorbed normalized continuum. Black horizontal lines mark the absorption edges for different components used for our equivalent width measurements. Relative ejection velocity of a component is the maximum velocity of a component measured with respect to the redshift of the C IV emission line. Redshift, epoch of observations and the peak radio flux density at 1.4 GHz for each source are also presented in each panel.

[3] In this work, we also refer to the BAL QSOs showing transient C IV components as transient BALs.

Table 1. Details of radio detected BALQSOs with multiple epoch spectroscopic observations in SDSS.

No.	Name	RA (h:m:s)	Dec (deg:m:s)	z_{em}	F_{int}^{FIRST} (mJy)	$\log(L_{radio})$ (ergs $s^{-1}Hz^{-1}$)	No. of Epochs	No. of Components	Comments[a]
1	SDSS J0014−0107	00:14:38.28	-01:07:50.19	1.8179	1.4	32.51	3	2	NV
2	SDSS J0041+0017	00:41:18.60	00:17:42.49	1.7667	0.9	32.28	5	1	V, red
3	SDSS J0046+0104	00:46:13.53	01:04:25.71	2.1551	3.0	33.02	5	3	V, Disappearance
4	SDSS J0053−0003	00:53:55.15	-00:03:09.35	1.7033	0.8	32.19	3	4	V, Odv
5	SDSS J0148−0051	01:48:12.81	-00:51:08.78	1.8189	3.2	32.86	2	4	V, blue
6	SDSS J0200−0845	02:00:22.00	-08:45:12.09	1.9423	7.8	33.32	2	3	NV
7	SDSS J0242+0104	02:42:24.02	01:04:52.57	2.4415	2.6	33.09	5	1	NV
8	SDSS J0743+3109	07:43:34.55	31:09:06.11	1.8983	1.7	32.64	2	3	V, Odv
9	SDSS J0803+5003	08:03:51.59	50:03:17.64	2.9472	13.4	33.99	4	3	NV
10	SDSS J0811+5007	08:11:02.88	50:07:24.60	1.8394	23.0	33.73	5	1	V, Disappearance
11	SDSS J0828+4452	08:28:04.55	44:52:56.99	2.9041	2.4	33.23	2	1	NV
12	SDSS J0835+4352	08:35:25.92	43:52:11.28	1.8218	1.7	32.59	2	1	V, blue
13	SDSS J0855+0809	08:55:28.08	08:09:36.10	1.7696	8.4	33.25	2	1	NV
14	SDSS J0929+3757	09:29:13.91	37:57:42.83	1.9021	43.1	34.04	2	1	NV
15	SDSS J0945+5055	09:45:13.91	50:55:21.71	2.1331	2.0	32.83	2	1	NV
16	SDSS J0956+4513	09:56:57.12	45:13:10.20	2.4091	1.7	32.89	2	2	NV
17	SDSS J0959+6333	09:59:30.00	63:33:59.76	1.8478	14.9	33.55	3	2	V, Disappearance
18	SDSS J1024+0940	10:24:27.35	09:40:29.81	1.8387	1.5	32.55	3	1	NV
19	SDSS J1044+1040	10:44:52.32	10:40:05.87	1.8823	16.4	33.61	2	6	V, Appearance,Odv
20	SDSS J1044+3656	10:44:59.52	36:56:05.27	2.8667	14.6	34.01	2	5	NV
21	SDSS J1105+1115	11:05:05.03	11:15:41.04	2.4531	2.1	32.99	2	2	NV
22	SDSS J1105+1512	11:05:31.43	15:12:15.84	2.0664	12.1	33.58	2	3	V, Appearance
23	SDSS J1113+0914	11:13:16.31	09:14:39.01	1.6738	1.2	32.35	2	4	NV
24	SDSS J1138+3704	11:38:03.12	37:04:03.00	1.8267	6.5	33.18	2	1	NV
25	SDSS J1149+3329	11:49:55.67	33:29:07.80	1.9124	1.7	32.64	2	1	NV
26	SDSS J1200+3508	12:00:51.59	35:08:31.56	1.6677	2.0	32.57	2	3	NV
27	SDSS J1217+3257	12:17:50.15	32:57:11.52	2.0420	1.4	32.63	2	1	NV
28	SDSS J1224+1010	12:24:10.56	10:10:31.07	1.9115	1.1	32.45	2	1	NV
29	SDSS J1303+0020	13:03:48.95	00:20:10.55	3.6487	1.1	33.13	2	3	NV
30	SDSS J1304+4210	13:04:25.44	42:10:09.83	1.8884	1.5	32.58	2	2	NV
31	SDSS J1318+1238	13:18:23.75	12:38:12.47	2.6304	2.2	33.09	2	1	NV, No CRTS
32	SDSS J1323−0038	13:23:4.559	-00:38:56.53	1.8260	8.9	33.31	4	3	NV
33	SDSS J1324+0133	13:24:07.92	01:33:13.21	2.5036	6.1	33.48	2	1	V, blue
34	SDSS J1331+0045	13:31:50.40	00:45:18.80	1.8953	2.9	32.87	2	1	NV
35	SDSS J1334−0123	13:34:28.08	-01:23:49.05	1.7941	3.6	32.90	2	1	NV
36	SDSS J1340+1232	13:40:14.87	12:32:18.23	1.9553	1.8	32.69	2	1	V, Odv
37	SDSS J1444+0033	14:44:34.80	00:33:05.35	2.0361	12.7	33.58	2	2	V, Odv
38	SDSS J1450+1233	14:50:55.92	12:33:31.31	2.7399	1.2	32.87	2	1	NV
39	SDSS J1503+4401	15:03:32.87	44:01:20.63	2.0435	10.0	33.48	3	2	NV, No CRTS
40	SDSS J1530+4409	15:30:49.68	44:09:56.87	1.7721	8.4	33.26	3	2	V, blue
41	SDSS J1532+4220	15:32:57.60	42:20:47.04	1.9595	1.1	32.48	2	2	NV
42	SDSS J1553+3245	15:53:55.44	32:45:13.32	2.0544	1.6	32.69	3	3	V
43	SDSS J1601+2947	16:01:38.40	29:47:34.44	1.9677	1.1	32.48	2	2	NV
44	SDSS J1603+3002	16:03:54.23	30:02:08.51	2.8321	53.7	34.56	2	1	NV
45	SDSS J1618+3301	16:18:12.96	33:01:55.91	2.0031	5.3	33.19	2	1	NV
46	SDSS J1621+3555	16:21:43.68	35:55:33.96	2.0646	1.2	32.57	2	3	NV
47	SDSS J1632+2201	16:32:39.36	22:01:41.87	1.9537	1.2	32.52	3	3	NV
48	SDSS J1641+3058	16:41:52.32	30:58:51.60	2.7687	2.1	33.13	2	3	NV
49	SDSS J1655+3945	16:55:43.19	39:45:19.80	1.7530	10.1	33.32	2	2	V, Disappearance
50	SDSS J2353−0050	23:53:13.68	-00:50:23.21	1.9588	1.2	32.52	2	1	NV

[a] V - variable BAL; NV - Non-variable BAL; red- red part of BAL varying; blue - blue part of BAL varying; Odv - variation in optical depth; Appearance - New BAL component appeared; Disappearance - BAL component disappeared.

SDSS J0046+0104, SDSS J0811+5007, SDSS J0959+6333 and SDSS J1655+3945 have atleast one C IV BAL component which disappeared in the later SDSS epoch and in SDSS J1044+1040 and SDSS J1105+1512 a new component is observed to have emerged in the later SDSS epoch. Filiz Ak et al. (2012) has already identified the BAL disappearance in SDSS J0811+5007. Interestingly, 5 out these six transient BAL sources have peak radio flux density at 1.4 GHz greater than 10 mJy. In the following section, we perform different statistical tests to understand the influence of the radio emitting plasma on the C IV outflows.

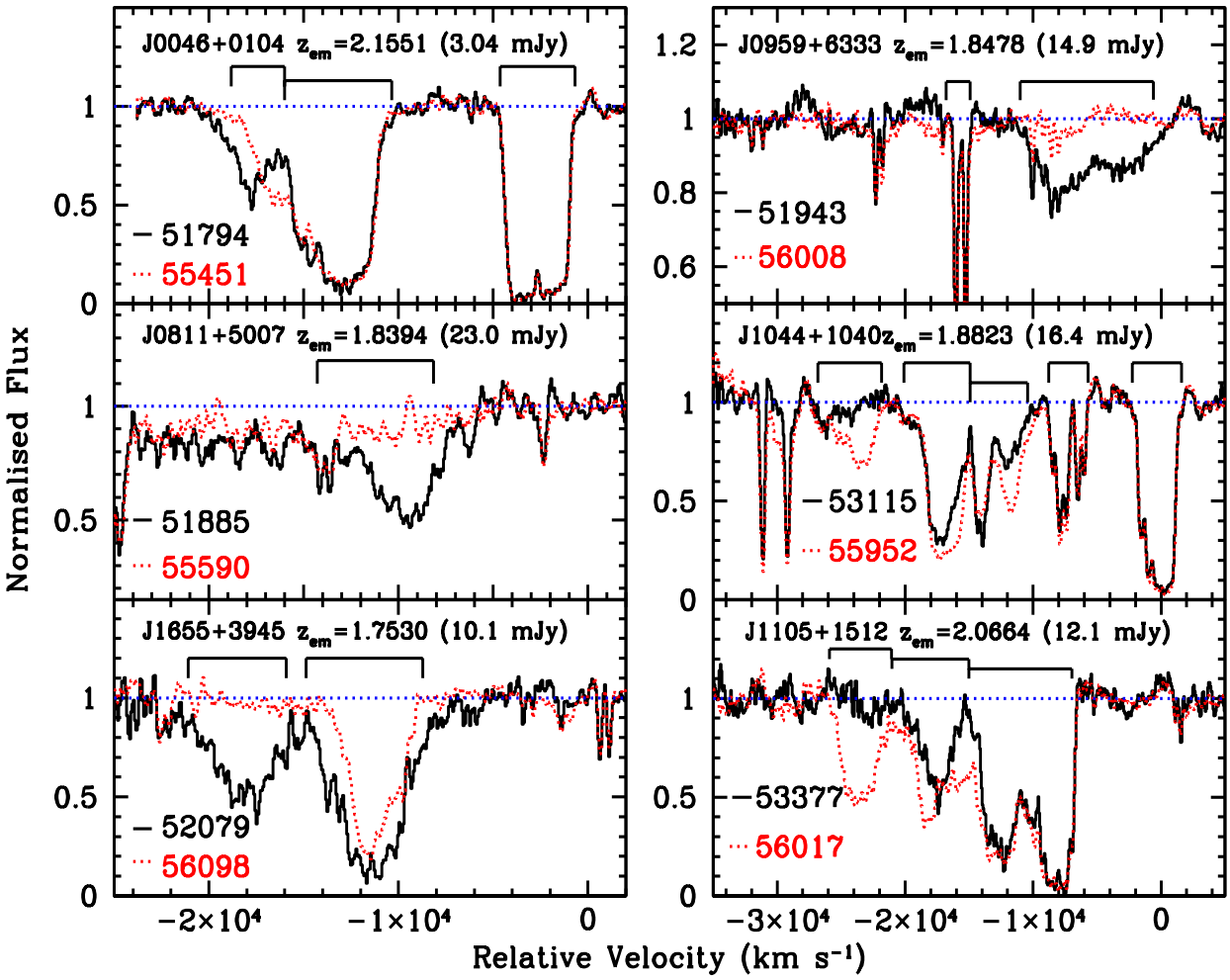

Figure 2. Normalized spectra of six sources showing transient C IV BALs. The spectra shown with dotted red line corresponds to later epoch measurements. The horizontal lines mark the velocity ranges for different components, identified by the method described in Fig 1, that are used for measuring the equivalent widths. Relative velocity is measured with respect to the centroid of the C IV emission line. Emission redshift, epoch of observations and the 1.4 GHz radio flux density from FIRST for each source are also provided.

5 STATISTICAL ANALYSIS

In this section, we investigate the correlations between the BAL variability and other properties of the sample. We use the absolute fractional variation in the C IV equivalent width of individual components to quantitatively characterise the BAL variability. Absolute fractional variation in the equivalent width is defined by $|\Delta W|/ < W >$ where ΔW and $< W >$ are the equivalent width differences and average equivalent width between two epochs respectively. This approach is particularly useful in studying the transient BAL cases where $|\Delta W|/ < W >$ close to 2 corresponds to a completely emerged or disappeared BAL component.

However for practical purpose, we define a BAL component to be a transient if the absolute fractional variation in the C IV equivalent width is greater than unity. This is because our definition of individual component may have included some additional absorption from gas unrelated to the transient component. All the 6 sources showing distinct C IV BAL transient signatures during our visual inspection are clearly selected when we impose this threshold. We compare properties of this transient C IV BAL sub-sample with the rest of the sample to understand the BAL transient phenomena. In particular, we wish to address whether there is any common observational correlations between cases with simple optical depth variability and the occurrence of new transient components.

5.1 Correlation with continuum parameters

Previous BAL variability studies have suggested that optical depth variations are not strongly correlated with continuum flux variations (Lundgren et al. 2007; Gibson et al. 2010; Vivek et al. 2014; Welling et al. 2014). In the case of Mg II emerging BALQSO SDSS J1333+0012, there is a suggestion that the emergence may be accompanied with continuum variations that can be interpreted as disturbances in the accretion disk causing the new emerging component

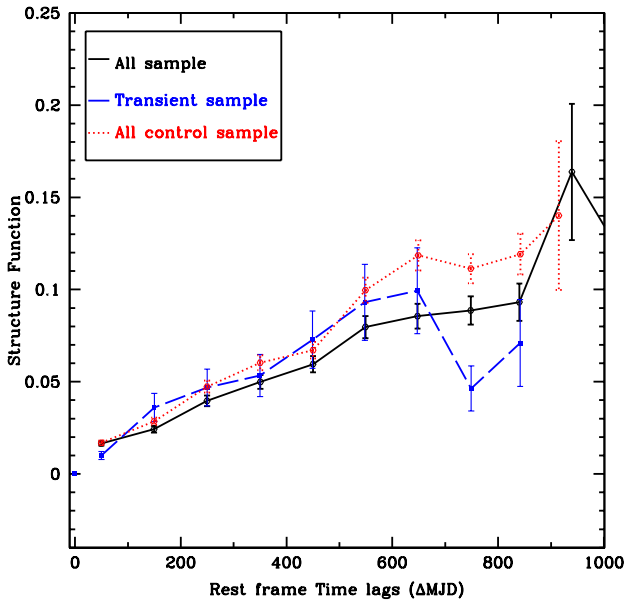

Figure 3. The black (solid), blue (dashed) and red (dotted) curves represent the structure function (in mag) of the CRTS magnitude variations of all the sources given in Table 1, C IV BALs with transient components in our sample and the radio quiet control sample respectively.

(Vivek et al. 2012a). In order to explore the role played by the continuum variations in the case of C IV BALs with transient components, it is important to compare the nature of continuum variability of these BALQSOs with the rest of the BALQSO population.

In this section, we address this using the structure function analysis of CRTS light curves. The structure function (SF) has been used extensively in the literature as a variability diagnostic for either individual or an ensemble of QSOs (Vanden Berk et al. 2004; Welsh et al. 2011; MacLeod et al. 2012). Several varying definitions of structure function have been used in literature which essentially quantify the amplitude of variability as the function of observed time-lags (See, Graham et al. 2014, for various definitions of SF).

For our present study, we have used the formulation of structure function and the associated error (SF_{err}) given by MacLeod et al. (2012):

$$SF = 0.74 * (IQR); \quad SF_{err} = SF * 1.15/\sqrt{(N-1)} \qquad (1)$$

where IQR is the 25%–75% interquartile range of the Δm distribution and N is the number of Δm values. We chose to bin the magnitude differences within intervals of 20 rest-frame time lag days before calculating the structure function. Welling et al. (2014) compared the structure functions of a sample of radio loud and radio quiet BALQSOs and reported similarity in the optical continuum variability between the two samples. Joshi & Chand (2013) also report a similarity in the microvariability (i.e., variability with in a day) properties of radio loud and radio quiet BALQSOs.

Fig. 3 shows the plot of absolute V-band magnitude variations at different time lags. The black solid, blue dashed and red dotted curve represents the structure function of the CRTS magnitude variability computed using Eq. 1 for all the QSOs in the sample, the transient BALQSOs in the sample and the radio quiet control sample respectively. It is clear that the variability properties of the QSOs with transient BALs and the rest are identical. The structure function of BAL QSOs with transient BAL component seems to be lower at time scales greater than 800 days. This would mean that BAL QSOs showing transient BAL component are less variable at longer time scales and is contrary to what is expected in the case of ionization driven outflows. This implies that the transient BAL phenomenon is most unlikely due to the ionization changes.

It is interesting to note that the SFs derived here are very much consistent with those of Welling et al. (2014) (see their Fig. 14). They found that the optical continuum variability of radio loud and radio quiet BALQSOs are similar in their sample. Therefore, we can conclude that overall optical variability of our radio detected BALQSO is also similar to that of radio quiet BALQSOs.

5.2 BAL transience and absorption line parameters

Previous BAL variability studies have found positive correlations of BAL variability with observed time-lag and ejection velocity, and a negative correlation with average equivalent width (Lundgren et al. 2007; Gibson et al. 2008, 2010; Capellupo et al. 2011; Filiz Ak et al. 2013; Vivek et al. 2014). In this section, we study the relationship between these quantities and transient C IV BAL phenomenon.

Fig. 4 shows the absolute fractional variation of C IV equivalent widths in individual absorption components with z_{em}, maximum velocity of the component, average C IV equivalent widths, mean depths of BAL components, rest-frame time lags and integrated radio luminosity. In each panel, the blue upper dashed and dotted horizontal lines represent a fractional variation of 2 and 1 respectively. The median value of the quantity in the abscissa is marked by the dashed magenta vertical line in each panel. Clearly there are six cases where the equivalent width fractional variation are between 2 and 1. In two cases, SDSS J0046+0104 and SDSS J0811+5007, the equivalent width fractional variation is close to 1. In the case of SDSS J0046+0104, the transient BAL component is weak and in the case of SDSS J0811+5007, the fractional variation values are suppressed by the inclusion of a small component in the high velocity end by our automatic algorithm. Panel (a) of Fig. 4 shows that there is no dependence of the occurrence of transient BAL on redshift. This is also confirmed by the two-sided Kolomogrov-Smirnov (KS) test results summarized in Table. 2.

From panel (b) in Fig. 4, it is clear that the fractional equivalent width change shows a large scatter at high maximum velocities. In particular absorption components that show change in fractional equivalent width in excess of 0.8 have ejection velocity in excess of 8000 kms^{-1}. All the 6 components identified as transient BALs have ejection velocities in excess of 11,000 kms^{-1}. This confirms that transient BAL phenomenon is more common among components with large ejection velocities. This is also confirmed by the KS-test results summarized in Table 2.

In panel (c) in Fig. 4 we plot fractional C IV equivalent

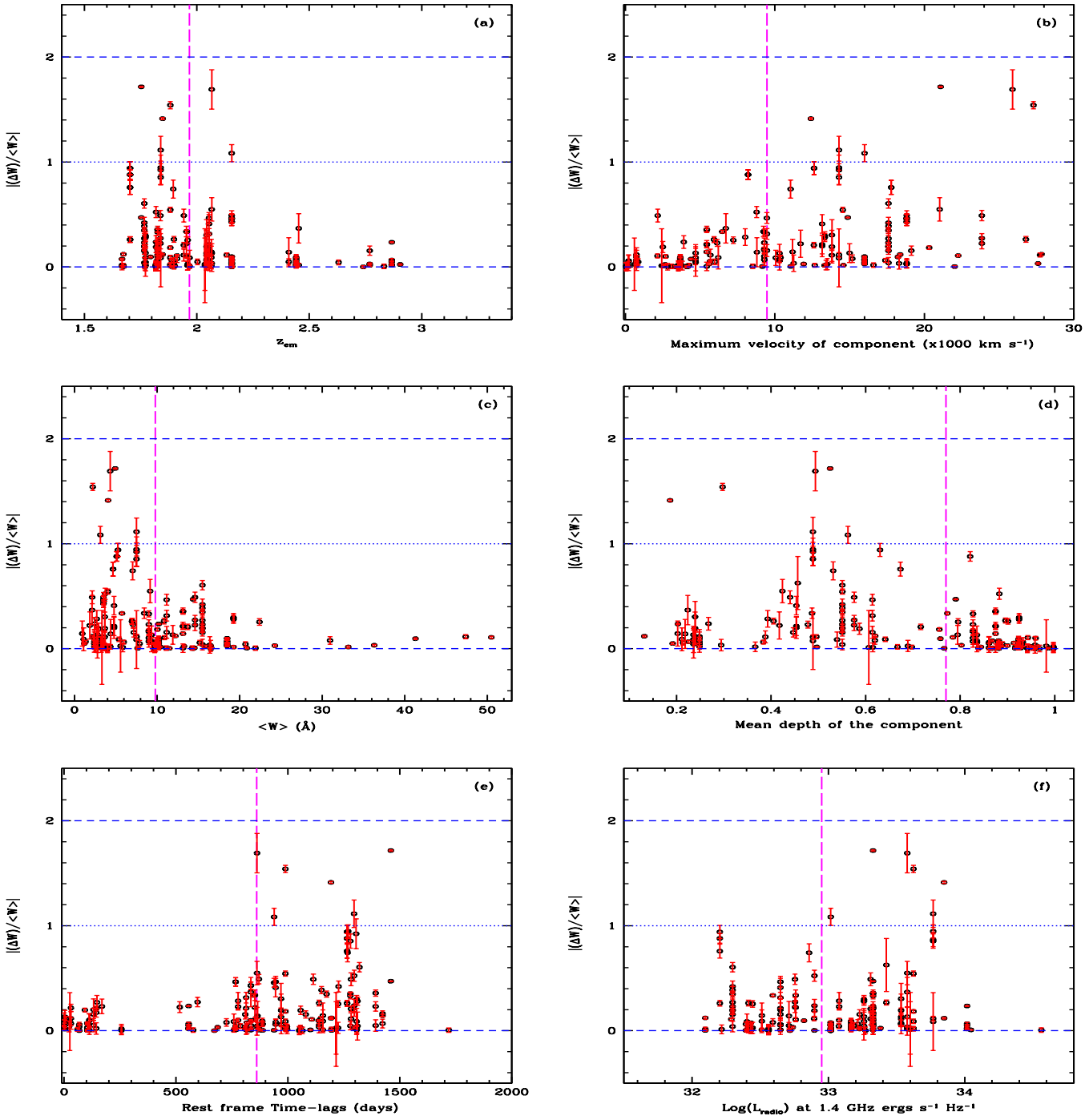

Figure 4. Absolute fractional variation of C IV equivalent widths of individual components are plotted against emission redshift, maximum velocity of the component, average equivalent width, mean depth, timelags and integrated radio luminosity. The upper blue horizontal dashed line represents a fractional variation of 2 which corresponds to a transient BAL component. The blue dotted horizontal line represents a fractional variation of 1. The median value of the distributions are marked by the vertical long dashed magenta line in each plot.

width as a function of mean C IV equivalent width. It is clear from the figure that the transient components tend to have the average C IV equivalent width less than 8 Å and mean depth of the C IV absorption trough less than 0.55 (see panel (d) of Fig. 4). This is consistent with the transient phenomenon occurring mainly in components that are typically shallow and have low equivalent widths. The low C IV equivalent width could either mean low covering factor or unsaturated absorption line.

It is clear from panel (e) in Fig. 4 that the envelope of fractional C IV equivalent width variations widens at long observed time-lags. In particular all the transient BAL com-

Table 2. Results of two-sided KS test for the parent radio detected BALQSO sample (60 objects) and the subsample of 6 transient BALQSOs

Parameter	D	$D^{\dagger}_{critical}$	p-value
Ejection velocity	0.40	0.34	0.01
Radio Luminosity	0.59	0.59	0.03
FIRST radio flux	0.63	0.59	0.01
Redshift	0.33	0.59	0.53
Timelags	0.18	0.22	0.17
Bolometric Luminosity	0.35	0.59	0.45
Eddington Ratio	0.18	0.59	0.99
M_{BH}	0.15	0.59	0.99
(SDSS r - WISE W4) color	0.53	0.59	0.07

† $D_{critical}$ values evaluated for a statistical significance, $\alpha = 0.05$

Table 3. Properties of transient BALs in the radio detected and radio quiet sample

No.	Name	Right Ascension	Declination	z_{em}	i (mag)	V^{a}_{eje} (kms^{-1})	ΔMJD^{b} (days)
Radio detected sample							
1	J0046+0104	00 46 13.54	+01 04 25.7	2.1551	-28.39	-18819.9	870.4
2	J0811+5007	08 11 02.90	+50 07 24.5	1.8394	-26.71	-14286.8	1279.1
3	J0959+6334	09 59 29.85	+63 34 00.2	1.8478	-29.11	-12410.4	1459.8
4	J1044+1040	10 44 52.41	+10 40 05.9	1.8823	-28.17	-27299.4	1192.4
5	J1105+1512	11 05 31.41	+15 12 15.9	2.0664	-27.35	-25897.6	975.2
6	J1655+3945	16 55 43.23	+39 45 19.9	1.7530	-27.45	-21089.9	861.9
Radio quiet control sample							
7	J0119+0043	01 19 48.52	+00 43 55.9	1.7668	-27.36	-2098.9	1341.7
8	J0825+2607	08 25 40.90	+26 07 37.4	1.7503	-27.13	-16119.9	1070.3
9	J0946+3800	09 46 02.23	+38 00 59.3	2.0678	-27.45	-25149.9	843.2
10	J1007+0304	10 07 16.69	+03 04 38.7	2.1241	-27.87	-18794.6	848.4
11	J1415+3956	14 15 33.99	+39 56 27.3	1.8270	-26.59	-18698.5	1042.2
12	J1448+1228	14 48 26.10	+12 28 14.7	2.0694	-27.19	-18987.0	814.2
13	J1636+2051	16 36 28.41	+20 51 21.6	1.7411	-27.19	-13735.3	813.1

^{a} V_{eje} is the ejection velocity of the transient component.
^{b} shortest rest-frame timescale over which the BAL transience observed.

ponents are seen at rest-frame timescales of more than 800 days.

In summary, we find that the transient C IV BAL phenomenon is more frequent in components with large ejection velocities having smaller C IV equivalent widths and monitored over a timescale of more than 800 days in the rest frame of the QSOs. This is similar to what was found by Filiz Ak et al. (2012) for disappearing C IV absorbers predominantly towards radio quiet QSOs. Interestingly the above found trend for the transient C IV BAL components are also seen for the general optical depth variability. Therefore, purely based on the discussions presented here the transient C IV BAL components may appear to be the extreme case of C IV variability (see Filiz Ak et al. 2013). In the following section, we investigate whether the frequency of occurrence of the transient C IV BAL components is significantly higher in the radio detected QSOs.

5.3 BAL transience and radio emission

We first noticed that the transient C IV BALs occur in sources with high integrated radio fluxes. While the two BALQSOs [4] with high radio flux density does not show a transient C IV absorption component, we find a tentative evidence for high fraction of transient C IV BAL components in BALQSO with flux density in excess of 10 mJy. To better characterize the intrinsic radio emission, we converted the integrated radio fluxes to luminosities. In panel (f) of Fig. 4 we plot the fractional equivalent width variations as a function of radio luminosity. It is apparent from this figure that the transient C IV BAL components predominantly occur in

[4] SDSS J0929+3757 and SDSS J1603+3002 have radio fluxes 43 mJy and 53 mJy respectively. In both these cases, C IV BALs are defined by one strong component (probably saturated) at low ejection velocities.

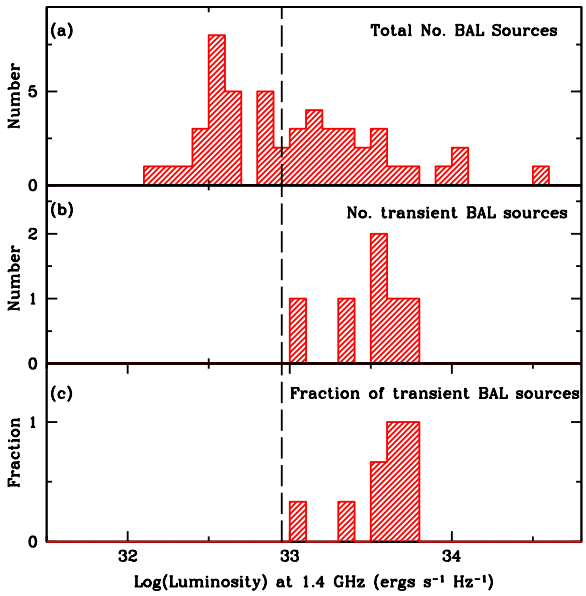

Figure 5. Radio luminosity distribution of C IV BALQSOs. The panels (a), (b) and (c) show the distribution for all the BALQSOs, transient BALQSOs and the fraction of transient BALQSOs, respectively. Black vertical dashed line corresponds to the median radio flux density of the sample.

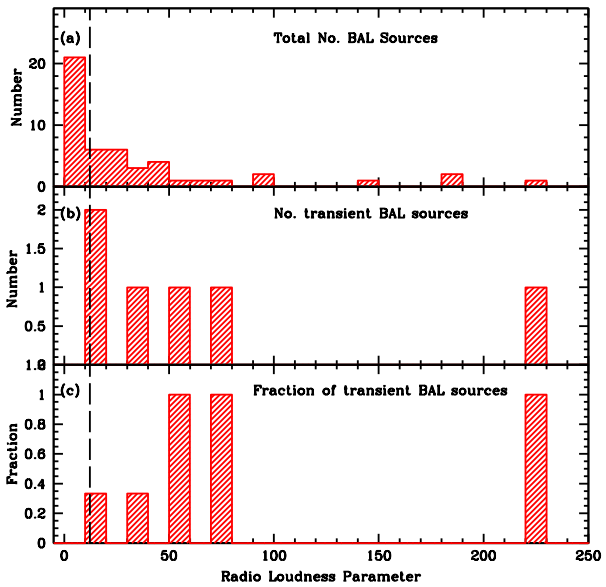

Figure 6. Radio loudness parameter distribution of C IV BALQSOs. The panels (a), (b) and (c) show the distribution for all the BALQSOs, transient BALQSOs and the fraction of transient BALQSOs, respectively. Black vertical dashed line corresponds to the median radio loudness parameter of the sample.

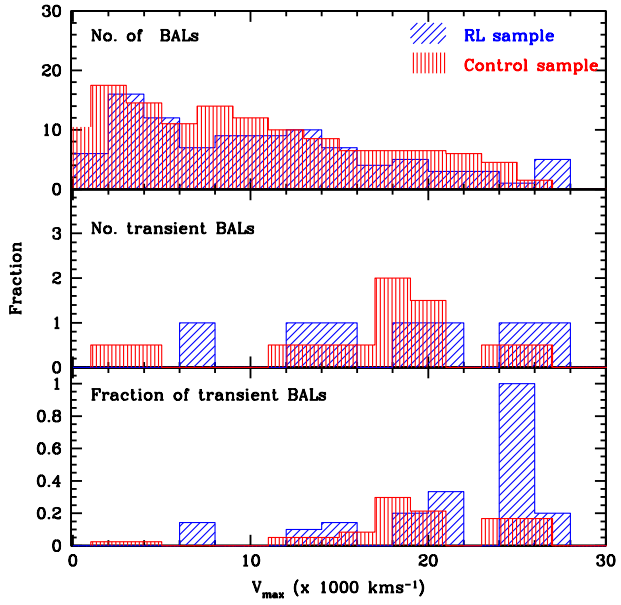

Figure 7. Histogram distribution of maximum ejection velocities of all the C IV BAL components. The blue (with slanted lines) and red (with vertical lines) histograms corresponds to the radio detected and radio quiet control sample respectively. *Top panel* : number of C IV BAL absorption components at each ejection velocity. *Middle panel* : number of transient C IV BAL components. *Lower panel* : the fraction of transient C IV BAL components .

radio bright sources. The KS-test results presented in Table 2 confirms that the radio flux/luminosity distributions in BALQSOs with transient C IV absorption are different from the rest of the QSOs.

This trend is also apparent in Fig. 5. In this figure, the top panel (a) shows the radio luminosity distribution of BALQSOs. The red (shaded) histogram in panel (b) shows the distribution of QSOs with a transient C IV BAL. Similarly, panel (c) shows the fraction of QSOs with transient C IV BALs in red. If we divide the sample into two at the median radio luminosity value (i.e, Log(L_{radio}) = 32.9 ergs s^{-1} Hz^{-1}), 25±10 % of sources with radio luminosity greater than the median show transient C IV BALs whereas none of the sources with radio luminosity less than the median show transient C IV BAL. Thus we have a tentative evidence (at 2.5 σ level) for the transient C IV BALs to be more probable in radio bright QSOs. Two sample KS tests between the transient and the parent sample shows that these two samples are different by 99%, 99% and 97% in their ejection velocity, radio flux density and radio luminosity distributions (see Table 2). Fig. 6 shows the distribution of radio loudness for BALQSOs. Clearly, all the C IV BALs with a transient component have radio loudness parameter greater than the median of the radio loudness parameter distribution, further confirming the result.

To explore this further, we consider the radio loud BAL sample of Welling et al. (2014). They estimated the 5 GHz radio luminosity for their sample using FIRST peak fluxes for the core, and integrated fluxes for the lobes, assuming radio spectral indices of α=−0.3 and −0.9, respectively. To make a straight-forward comparison with our sample, we

consider the compact (unresolved in FIRST) BALQSOs in their sample having the 5 GHz radio luminosity (in log) > 32.7. For α=−0.3 this corresponds to a $\log(L_{radio}) = 32.9$ at 1.4 GHz i.e. the median value for our sample. Thus, considering only compact BALQSOs in the two samples with $\log(L_{radio}) \geqslant 32.9$ at 1.4 GHz, we find that the fraction of transient BALs in our and their samples are 27% and 10% respectively. While the difference could simply be due to the small number statistics, we notice that not all QSOs in the sample of Welling et al. (2014) are monitored for > 800 days i.e. the timescale over which most of the transient C IV absorption occur in our sample. For example, only 5 out of 21 compact BALQSOs with $\log(L_{radio}) = 32.9$ at 1.4 GHz in the their sample are monitored over a rest frame time-scale of greater than 800 days. The two sources showing possible transience are among them i.e. a detection rate of 40±28 %. In our radio detected sample, there are 20 sources with $\log(L_{radio}) \geqslant 32.9$ at 1.4 GHz and rest-frame timescales $\geqslant$ 800 days. Six out of this 20 sources show transient nature (i.e., detection rate of 30±12 %). Thus, with in statistical uncertainties, there is no major discrepancy in the transient BAL detection rate between our sample and the sample of Welling et al. (2014) as long as we confine to similar monitoring periods. This exercise also establishes the importance of long time-scale monitoring in addition to having large enough sample to have statistically significant results.

To further investigate the finding of 'higher' fraction of transient C IV BALs at high radio flux densities/luminosities in our sample, we proceed to study the fraction of transient C IV BAL sources in radio quiet BALQSOs. A clear deviation from the radio detected sample will firmly establish the role played by the radio jets in driving the transient BALs. For this, we constructed a control sample of radio quiet BALQSOs that have multiple epoch spectra in SDSS DR10. For each QSO with transient C IV absorption in the radio detected sample, we constructed a control sample of 10 radio quiet BALQSOs matching closely in absolute i-band magnitude and redshift. We first generated a sample of 20-25 radio quiet BALQSOs which are closest in redshift and absolute i-band magnitude for each source in the radio detected transient C IV sample. From this sample, we then selected 10 sources for each transient C IV BALQSO which has multiple epoch spectra in SDSS DR10. The typical dispersion in the Δz and Δi magnitude values of the control sample is 0.02 and 0.2 respectively except for the case of J0959+6334 where it is 0.08 and 0.3. Each of these 60 sources in the control sample were first visually inspected for the presence of transient C IV BAL components. We then, followed the procedure described in Section 3 to identify the transient C IV BAL components[5]. Among the 60 sources in the control sample, 7 sources (i.e. 12±4 %) show clear transient C IV features. This is close to 12±5 % we find for our full radio detected sample with out applying any monitoring timescale cuts. Next, we consider only sources that are monitored over a period more than 800 days in the QSO's rest frame in both our's and the control sample. We find the transient detection rate of 23±9 % and 18±7 % for our and control sample respectively. This is also consistent within errors. The two rates are consistent with one another and roughly 30% smaller than the detection rate we found for QSOs with $\log(L_{radio}) > 32.9$. However, the errors are too large to clearly favor radio brightness being an important driver of transient BAL flows.

As ejection velocity is also an important quantity in the problem, we need to make sure the distribution of ejection velocity in the control sample is not very different from our radio detected sample. Table 3 gives a list of all the transient C IV BALQSOs identified in this study including those in the control sample. The ejection velocity distributions of the radio detected and control sample BALQSOs are found to be similar. KS test between the two samples gives a D value of 0.13 and probability of 0.28. KS test between the transient C IV in the radio detected sample and the control sample gives the D and probability values of 0.3 and 0.06 respectively. The similarity of ejection velocity distributions in the above three samples ensures that the transient C IV BAL phenomena in the control sample sources are not enhanced by the bias in the distribution of ejection velocity. The lack of very strong correlation between the transient C IV BAL and the radio properties seem to suggest that there is no observable dependence between radio jets and transient C IV absorbing flows in QSOs.

Fig. 7 gives a more clear picture of the trend with the ejection velocity. In the figure, the top panel represents the histogram distribution of all the BAL components in the radio detected sample (blue/with slanted lines) and radio quiet control sample (red/with vertical lines). The middle panel presents the distribution of the transient C IV components and the lower panel represents the fraction of transient C IV BALs. It is clear that the fraction is high at higher velocities for both the radio detected and radio quiet control sample. We also note that the ratio of ejection velocity of the transient component to the maximum ejection velocity of the BALs peaks at unity. The transient C IV components are more likely to be with higher ejection velocities. We also checked if any preferential time sampling of sources is the reason for the BAL transience in some of the sources in the sample. Two-sided KS test for the transient and parent sample rest-frame time lag distributions result in D and probability values of 0.18 and 0.17 respectively. This implies that the time-sampling of the sources with transient BALs is nothing special compared to the other BALQSOs in the sample.

5.4 BAL transience and various derived QSO parameters

To investigate further whether basic properties of QSOs showing transient C IV BAL (both in our parent and control sample) is different from the rest of the BALQSOs, we matched the sources in this study with those in the SDSS DR7 QSO properties catalogue of Shen et al. (2011) to explore the correlation of transient C IV BALs with different inferred QSO properties. This catalogue covers all the sources in this study except for one non-transient source each in the radio detected and the control sample. Fig. 8 shows the

[5] Fig.A2 shows the absolute fractional variation of C IV equivalent widths in the individual absorption components of the control sample sources with z_{em}, maximum velocity of the component, average equivalent widths and rest-frame time lags. We also find that our control sample BALQSOs exhibit all the known correlations between BAL variability and various absorption line parameters discussed in Section 5.2.

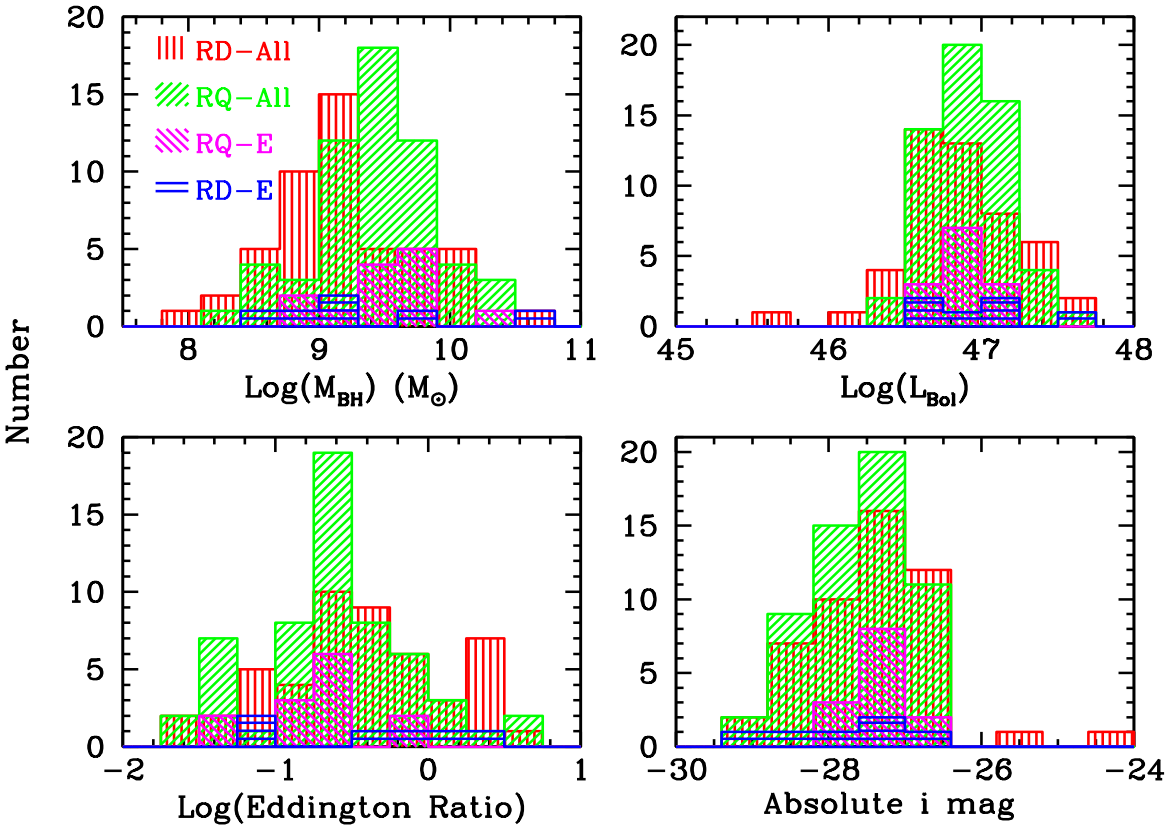

Figure 8. Histogram distribution of the quasar properties, Eddington ratio, mass of the blackhole, bolometric luminosity and absolute i-band magnitude for various samples in the study. *Red histogram with vertical lines* : radio detected sample, *green histogram with 45° slanted lines* : radio quiet control sample, *blue histogram with horizontal lines* : radio detected transient sample, *magenta histogram with -45° slanted lines* : radio quiet transient sample.

histogram distributions of the QSO properties: Eddington ratio, blackhole mass, bolometric luminosity and absolute i-band magnitude for the four samples in this study. The red (with vertical lines), green (with 45° slanted lines), blue (with horizontal lines) and magenta (with -45° slanted lines) histograms represent the radio detected, radio detected transient, radio quiet, radio quiet transient sample. There is no evidence for any correlation between the transient C IV BALs with any of the above mentioned QSO properties. Results of KS tests also reveal that different samples in this study belong to the same 'general' QSO population (see Table 2).

5.5 Correlation with IR properties

We measure the far-infrared fluxes of our sources from WISE (Wide-field Infrared Survey Explorer) catalogue. WISE operates in four wavelength bands W1, W2, W3 and W4 which are centered at 3.4, 4.6, 12 and 22 microns respectively. We use fluxes in these bands to probe the role of dust in the transient outflows. Recently, Zhang et al. (2014) explored the role of dust in driving the outflows in a sample of 2099 BALQSOs. They find that the outflow strength and velocity is strongly correlated with the near infrared continuum slope which is a good indicator of dust emission. They proposed a dusty outflow scenario to explain the observed correlations between the near-infrared continuum slope and BAL strength. In this scenario, dusty clouds emerging from the outer regions of the accretion disk or innermost regions of the torus, are uplifted above the disk and exposed to the central engine. While the low density part of this cloud is highly ionized and is responsible for blue-shifted absorption lines, the high density part holds the dust and radiates in the NIR.

Several earlier studies in the literature have made use of a selection criteria in the SDSS-WISE colors to pick dust obscured quasars. Hot dust emission dominates the rest-frame SED of a QSO > 3 μm. Our sample has a minimum and maximum emission redshift of 1.67 and 3.63 with a median at 1.91. WISE W4 magnitude clearly traces the dust emission for the redshift range of our sample. In this study, we use the SDSS r - WISE $W4$ color as a proxy for the strength of dust emission. Photometric spectral index values given in the SDSS catalogue can also be used as a measure of the reddening parameter. Fig. 9 gives the histogram distributions of the four samples in this study, namely radio detected sample (red with -45° slanted lines), radio quiet control sample (green with horizontal lines), radio quiet transient C IV sample (magenta with 45° slanted lines) and the radio detected transient C IV sample (blue filled). From Fig. 9, there is no clear evidence for the role of dust in driving the transient C IV BALs. Two sided KS test (see Table 2) for the radio

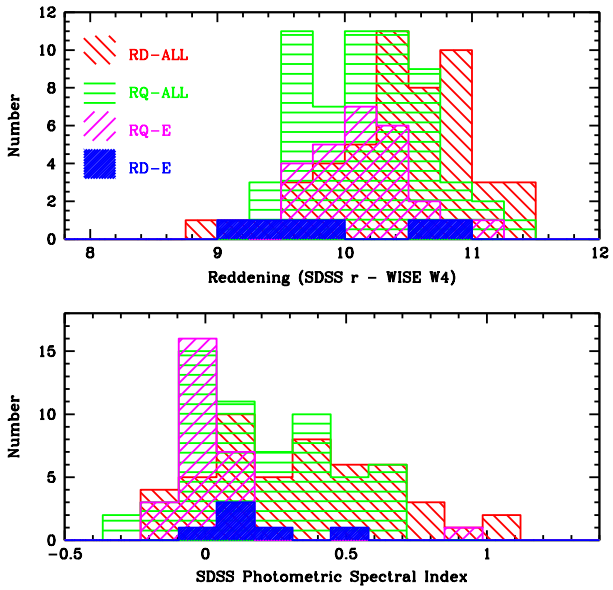

Figure 9. Distribution of two parameters characterising reddening of the BALQSOs. *upper panel*: Reddening characterised by SDSS r - WISE W4 color. *lower panel*: Reddening characterised by the SDSS photometric spectral index. The four samples in this study are radio detected sample (red with -45° slanted lines), radio quiet control sample (green with horizontal lines), radio quiet transient C IV sample (magenta with 45° slanted lines) and the radio detected transient C IV sample (blue filled).

detected and transient C IV BAL sample also does not point to any clear connection between the presence of dust and transient BAL phenomenon. Here again, we caution that our sample of radio detected BAL quasars is much smaller compared to the Zhang et al. (2014) sample.

6 DISCUSSION & SUMMARY

Recent studies have revealed that the radio properties of BAL and non-BALQSOs are more alike than different. Rawlings & Jarvis (2004) have found that whenever powerful jets are triggered, there is a dramatic increase in the efficiency of the feedback. It is quite possible that the onset of radio jets can have a feedback on to the accretion processes, which may trigger or quench the outflows. The transient C IV BAL systems in quasars can be used to determine the exact physical conditions prevailing at the time of outflow being ejected or quenched.

We have presented a detailed analysis of BAL variability for a sample of radio detected BALQSOs in the SDSS DR10 spectroscopic survey, with an emphasis on the transient C IV BALs. In the overall sample of radio detected sources, the fraction of transient C IV BAL sources (12%) is higher than what is found (3.3%) by Filiz Ak et al. (2012) for disappearing C IV BALs. This may be due to the the higher rest-frame observation timescales for our sample (6.5 yr) as compared to Filiz Ak et al. (2012) sample (3.9 yr). This fraction is large (25%) among the higher radio flux density sources in our sample. However, we notice that the occurrence of transient BALs in Welling et al. (2014) is not as high as this value. We show that the difference is mainly due to differences in the monitoring period of the two sample. When sub-samples are constructed with monitoring period larger than 800 days in the QSO rest-frame, we do find higher detection rates even in the sample of Welling et al. (2014). Using a control sample of radio quiet BALQSOs matched to the QSOs showing transient C IV BALs in radio detected QSOs, we find 12% cases showing transient C IV BAL troughs. This is consistent with the overall rate found for radio detected sources. Our control sample also hints on the occurrence of transient BALs being slightly higher in the case of radio bright QSOs. However, this difference is not overwhelmingly high and cannot be demonstrated at high statistical significance with the present data.

Radio detected BALQSO sample in this study also follows various BAL variability trends already known for C IV and Mg II BALs. Notable is the trend with the outflow velocity. The transient C IV BALs most often occur at higher outflow velocities, typically greater than 10000 kms^{-1}. We also find that the transient BAL components are more frequently detected for rest-frame timescales of 800 days. This could either mean a characteristic timescale over which the ionization changes or the cloud crossing time across our line of sight. There is no correlation found between the transient BALs and optical continuum parameters. So, ionization changes in the outflowing gas due to the changing continuum is most unlikely driver for the transient phenomena. However, it is possible that the optical continuum variation inferred with CRTS lightcurves obtained without a specific filter may not be an ideal tracer of the ionizing continuum. We also do not find any correlations between the occurrence of transient C IV BALs and various other QSO properties like Eddington ratio, black hole mass and luminosity.

We use the characteristic ejection velocities (i.e > 10000 kms^{-1}) and timescale ($\sim$ 800 days) of the transient flow with a simple model proposed by Hall et al. (2011) to place average constraints on the location and transverse speed of C IV emerging BAL components. Following Hall et al. (2011) , we estimate the diameter of the disc within which 90 per cent of the 2700 $\AA$ continuum is emitted to be $D_{2700} \sim 2 \times 10^{16}$ cm for the typical black hole of mass $10^9 M\odot$ for our sample. This, together with the characteristic BAL transience time scale of 800 rest frame days results in a transverse velocity of 3100 kms^{-1}. We assume a typical line of sight (LOS) velocity of 1×10^4 kms^{-1}for our calculations. Section 4.3 and 4.4 of Hall et al. (2011) give a model for constraining the BAL structure location. The exact estimate of the location of the flow requires the knowledge of the angle of LOS λ and the angle of the velocity vector θ above the accretion disc. As we are interested in the average properties, we computed the location of the BAL outflow for each combination of λ and θ and then averaged it. Following the procedure of Hall et al. (2011), we obtain an estimate of BAL launching radius to be 0.5$\pm$0.001 pc and the distance d_{BAL} from the black hole to be 2.2$\pm$0.1 pc. This is just outside the broad line region ($\sim$ 1 pc) for a typical quasar of $\log(L_{bol}) = 46.8$ ergs s^{-1}. Thus, the flow has not yet reached ISM to provide a strong feedback on the star formation.

In the absence of clear evidences for any correlations between the occurrence of transient C IV BALs and various parameters explored here, it is probable that transient BAL phenomenon is just an extension of normal BAL variability.

Similar optical continuum variability and BAL transience properties of radio detected and radio quiet BAL QSO samples might suggest that radio detected BAL QSOs are not necessarily always viewed down the jet axis. Our results do not support the case of jet-cloud interactions triggering bulk motions in the BAL outflow that can be seen in the form of transient BAL components. We also realize that the number transient BALs in our sample is too small to extract any possible weak dependences. A similar study with a larger sample size is needed to completely understand the transient BAL phenomenon. This study increases the sample size of transient BALQSOs by 18. Future spectroscopic monitoring of these sources will allow us to look for further dynamical evolution in these BALs. Multi wavelength observations of these sources will help to understand the role of changing 'sheilding gas' in driving transient BAL phenomenon. Ongoing and future spectroscopic surveys like eBOSS (extended Baryon Oscillation Spectroscopic Survey), LAMOST (Large Sky Area Multi-Object Fibre Spectroscopic Telescope) look promising for identifying new transient BAL sources and understanding the physical mechanism driving the transient phenomenon.

ACKNOWLEDGEMENTS

We thank the anonymous referee for a thorough review and helpful comments which led to an improved manuscript. Funding for SDSS-III has been provided by the Alfred P. Sloan Foundation, the Participating Institutions, the National Science Foundation, and the U.S. Department of Energy Office of Science. The SDSS-III web site is http://www.sdss3.org/.

SDSS-III is managed by the Astrophysical Research Consortium for the Participating Institutions of the SDSS-III Collaboration including the University of Arizona, the Brazilian Participation Group, Brookhaven National Laboratory, Carnegie Mellon University, University of Florida, the French Participation Group, the German Participation Group, Harvard University, the Instituto de Astrofisica de Canarias, the Michigan State/Notre Dame/JINA Participation Group, Johns Hopkins University, Lawrence Berkeley National Laboratory, Max Planck Institute for Astrophysics, Max Planck Institute for Extraterrestrial Physics, New Mexico State University, New York University, Ohio State University, Pennsylvania State University, University of Portsmouth, Princeton University, the Spanish Participation Group, University of Tokyo, University of Utah, Vanderbilt University, University of Virginia, University of Washington, and Yale University.

REFERENCES

Bautista, M. A., Dunn, J. P., Arav, N., Korista, K. T., Moe, M., & Benn, C., 2010, ApJ, 713, 25

Borguet, B. C. J., Arav, N., Edmonds, D., Chamberlain, C., & Benn, C., 2013, ApJ, 762, 49

Bruni, G., Dallacasa, D., Mack, K.-H., Montenegro-Montes, F. M., González-Serrano, J. I., Holt, J., & Jiménez-Luján, F., 2013, A&A, 554, A94

Bruni, G., Mack, K.-H., Salerno, E., et al., 2012, A&A, 542, A13

Capellupo, D. M., Hamann, F., Shields, J. C., Rodríguez Hidalgo, P., & Barlow, T. A., 2011, MNRAS, 413, 908

Dawson, K. S., Schlegel, D. J., Ahn, C. P., et al., 2013, AJ, 145, 10

DiPompeo, M. A., Brotherton, M. S., & De Breuck, C., 2012, ApJ, 752, 6

Drake, A. J., Djorgovski, S. G., Mahabal, A., et al., 2009, ApJ, 696, 870

Dunn, J. P., Bautista, M., Arav, N., et al., 2010, ApJ, 709, 611

Filiz Ak, N., Brandt, W. N., Hall, P. B., et al., 2012, ApJ, 757, 114

—, 2013, ArXiv e-prints

Gawronski, M. P. & Kunert-Bajraszewska, M., 2011, ArXiv e-prints

Germain, J., Barai, P., & Martel, H., 2009, ApJ, 704, 1002

Ghosh, K. K. & Punsly, B., 2007, ApJ, 661, L139

Gibson, R. R., Brandt, W. N., Gallagher, S. C., Hewett, P. C., & Schneider, D. P., 2010, ApJ, 713, 220

Gibson, R. R., Brandt, W. N., Schneider, D. P., & Gallagher, S. C., 2008, ApJ, 675, 985

Graham, M. J., Djorgovski, S. G., Drake, A. J., Mahabal, A. A., Chang, M., Stern, D., Donalek, C., & Glikman, E., 2014, MNRAS, 439, 703

Gregg, M. D., Becker, R. H., & de Vries, W., 2006, ApJ, 641, 210

Hall, P. B., Anosov, K., White, R. L., Brandt, W. N., Gregg, M. D., Gibson, R. R., Becker, R. H., & Schneider, D. P., 2011, MNRAS, 411, 2653

Hamann, F., Kaplan, K. F., Rodríguez Hidalgo, P., Prochaska, J. X., & Herbert-Fort, S., 2008, MNRAS, 391, L39

Hopkins, P. F., Murray, N., & Thompson, T. A., 2009, MNRAS, 398, 303

Jiang, D. R. & Wang, T. G., 2003, A&A, 397, L13

Joshi, R. & Chand, H., 2013, MNRAS, 429, 1717

Krongold, Y., Binette, L., & Hernández-Ibarra, F., 2010, ApJ, 724, L203

Kunert-Bajraszewska, M., Cegłowski, M., Katarzyński, K., & Roskowiński, C., 2015, A&A, 579, A109

Kunert-Bajraszewska, M. & Marecki, A., 2007, A&A, 469, 437

Leighly, K. M., Hamann, F., Casebeer, D. A., & Grupe, D., 2009, ApJ, 701, 176

Liu, Y., Jiang, D. R., Wang, T. G., & Xie, F. G., 2008, MNRAS, 391, 246

Lundgren, B. F., Wilhite, B. C., Brunner, R. J., Hall, P. B., Schneider, D. P., York, D. G., Vanden Berk, D. E., & Brinkmann, J., 2007, ApJ, 656, 73

Ma, F., 2002, MNRAS, 335, L99

MacLeod, C. L., Ivezić, Ž., Sesar, B., et al., 2012, ApJ, 753, 106

Moe, M., Arav, N., Bautista, M. A., & Korista, K. T., 2009, ApJ, 706, 525

Montenegro-Montes, F. M., Mack, K.-H., Benn, C. R., Carballo, R., González-Serrano, J. I., Holt, J., & Jiménez-Luján, F., 2009, Astronomische Nachrichten, 330, 157

Pâris, I., Petitjean, P., Aubourg, É., et al., 2014, A&A, 563, A54

Proga, D., Rodriguez-Hidalgo, P., & Hamann, F., 2012, in

Astronomical Society of the Pacific Conference Series, Vol. 460, AGN Winds in Charleston, Chartas, G., Hamann, F., & Leighly, K. M., eds., p. 171
Rawlings, S. & Jarvis, M. J., 2004, MNRAS, 355, L9
Rodríguez Hidalgo, P., Hamann, F., & Hall, P., 2011, MNRAS, 411, 247
Shen, Y., Richards, G. T., Strauss, M. A., et al., 2011, ApJS, 194, 45
Vanden Berk, D. E., Wilhite, B. C., Kron, R. G., et al., 2004, ApJ, 601, 692
Vivek, M., Srianand, R., Mahabal, A., & Kuriakose, V. C., 2012a, MNRAS, 421, L107
Vivek, M., Srianand, R., Petitjean, P., Mohan, V., Mahabal, A., & Samui, S., 2014, MNRAS, 440, 799
Vivek, M., Srianand, R., Petitjean, P., Noterdaeme, P., Mohan, V., Mahabal, A., & Kuriakose, V. C., 2012b, MNRAS, 423, 2879
Welling, C. A., Miller, B. P., Brandt, W. N., Capellupo, D. M., & Gibson, R. R., 2014, MNRAS, 440, 2474
Welsh, B. Y., Wheatley, J. M., & Neil, J. D., 2011, A&A, 527, A15
Weymann, R. J., Morris, S. L., Foltz, C. B., & Hewett, P. C., 1991, ApJ, 373, 23
White, R. L., Helfand, D. J., Becker, R. H., Glikman, E., & de Vries, W., 2007, ApJ, 654, 99
Zhang, S., Wang, H., Wang, T., Xing, F., Zhang, K., Zhou, H., & Jiang, P., 2014, ApJ, 786, 42

APPENDIX A: CONTROL SAMPLE : EMERGING SAMPLE

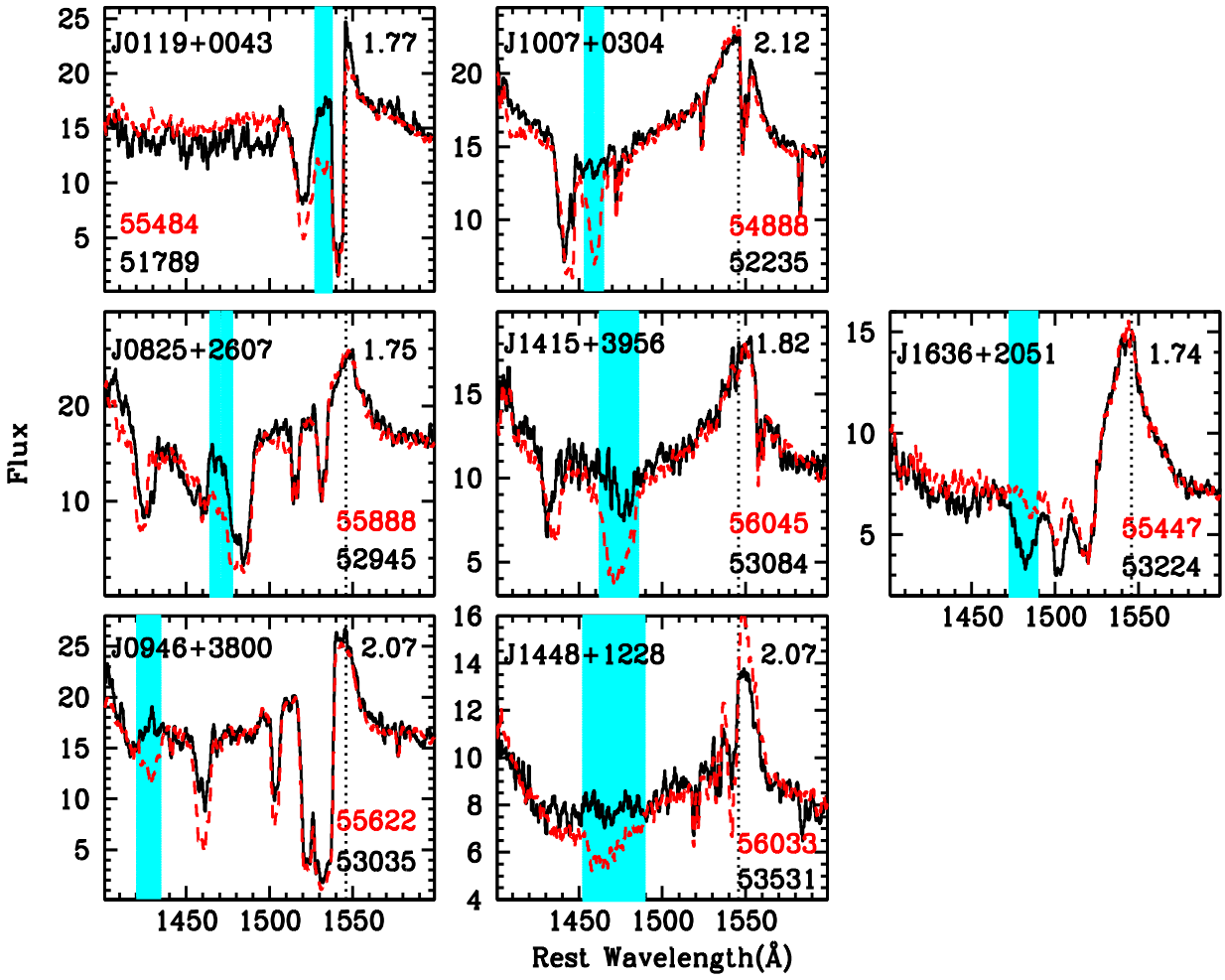

Figure A1. Spectra of control sample sources showing BAL appearance/disappearance. Red dashed spectra correspond to later epoch measurements. Shaded region represents the transient components. Relative velocity is measured from the C IV emission line. Redshift, epoch of observations for each source are also marked.

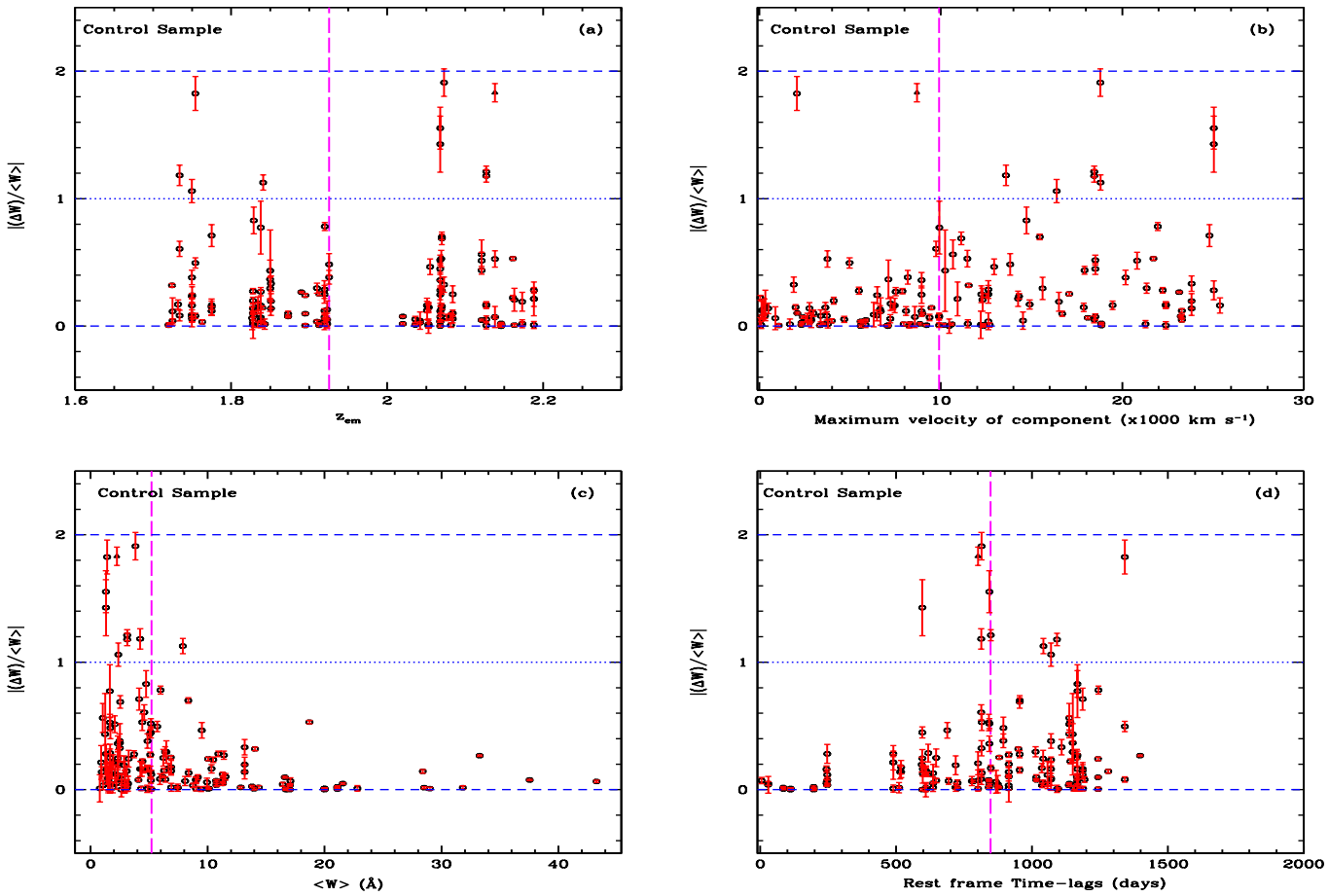

Figure A2. Absolute fractional variation of C IV equivalent widths of the control sample sources are plotted against emission redshift, maximum velocity of the component, fractional equivalent width variation, and rest-frame timelags. The upper blue horizontal dashed line represents a fractional variation of 2 which corresponds to emergence of BAL. The blue dotted horizontal line represents a fractional variation of 1. The median value of the distributions are marked by the vertical long dashed magenta line in each plot.